Journal of Alloys and Compounds 489 (2010) 297–303

Contents lists available at ScienceDirect

Journal of Alloys and Compounds

journal homepage: www.elsevier.com/locate/jallcom

A flexible microwave absorber based on nickel ferrite nanocomposite

Vijutha Sunny[a], Philip Kurian[b], P. Mohanan[c], P.A. Joy[d], M.R. Anantharaman[a,*]

[a] Department of Physics, Cochin University of Science and Technology, Kochi 682 022, India
[b] Department of Polymer Science and Rubber Technology, Cochin University of Science and Technology, Kochi 682 022, India
[c] Department of Electronics, Cochin University of Science and Technology, Kochi 682 022, India
[d] Physical Chemistry Division, National Chemical Laboratory, Pune 411 008, India

ARTICLE INFO

Article history:
Received 6 June 2009
Received in revised form
11 September 2009
Accepted 15 September 2009
Available online 23 September 2009

Keywords:
Nickel ferrite
Nanocomposites
Cavity perturbation
Complex permittivity
Complex permeability
Microwave absorber

ABSTRACT

Flexible magnetic composite materials were prepared by incorporating precharacterized nickel ferrite nanoparticles in a natural rubber matrix. The complex dielectric permittivity and magnetic permeability of the composites were measured at different microwave frequencies using the cavity perturbation technique. A steady increase in dielectric permittivity was observed with increase in filler concentration. Maxwell-Garnett mixture equations were employed to model the effective permittivity and permeability of the composite. Reflection loss was estimated by employing the model of single layer absorber backed with a perfect conductor. Reflection loss minima of −5.9 dB at 3.2 GHz for 12 mm thick rubber ferrite composite sheet is obtained in the S-band while a loss up to −16 dB could be achieved at 9.5 GHz in the X-band.

1. Introduction

Flexible microwave absorbers are thought to be ingenious new generation materials having potential applications in wireless data communication, local area network, satellite television and heating systems [1]. Ferrites of different composition have been widely studied because of their potential in finding numerous applications in electronic devices [2–5]. There is an increasing demand for cost effective electromagnetic absorber technology with minimal electromagnetic pollution and electromagnetic interferences. An ideal microwave absorber is characterized by a reflection loss less than −20 dB. For a material of optimum thickness, the impedance matching condition [6,7] depends on the complex relative dielectric permittivity ($\varepsilon_r = \varepsilon' - j\varepsilon''$) and complex relative magnetic permeability ($\mu_r = \mu' - j\mu''$) at the frequency of interest. Tuning of these two parameters along with the manipulation of thickness would aid in obtaining a high performance microwave absorber.

Nickel ferrite has been widely used in microwave devices and in electromagnetic shields due to its chemical stability, corrosion resistance and high saturation magnetization in addition to its microwave absorbing properties. Rubber ferrite nanocomposites (RFCs) can play an important role here in realizing these microwave absorbers with additional functionalities like elasticity and moldability aided by light weight [2,8,9]. Moreover, the dielectric and magnetic properties of the nanocomposites can be tailored by using the right amount of the filler in a single shot. Tuning the imaginary part of permeability μ'' improves matching, broaden the range of operating frequencies, increase attenuation and reduce the thickness of absorber layer. This can be achieved by using appropriate fillers with optimum magnetic permeability.

Natural rubber is a low cost material and its processing technique [10] is a well developed and matured technology. Nickel ferrite as filler fits into the requirement of having the appropriate permeability, low loss and low dc conductivity. High resistivity ($\sim 10^{14}$ times that of metal) ensures low eddy current loss in high frequency regime [11]. Further, the Curie temperature of nickel ferrite is ~858 K which makes them ideal for high temperature applications. Low coercivity and high saturation magnetization of nickel ferrite are also significant for obtaining good absorption properties. It has been reported that in the nanoregime, the dielectric permittivity and magnetic permeability of ferrites gets considerably modified with respect to their ceramic counterparts because of their high surface to volume ratio [2–5]. Hence incorporation of nickel ferrite nanoparticles into a matrix like natural rubber can result in an excellent microwave absorbing material.

Although physico-mechanical properties of natural rubber composites are extensively studied, their microwave properties are not completely exploited. Proper understanding of the dielectric and magnetic behaviour of polymer composites at high frequencies will help in engineering new materials for applications. Incorpo-

* Corresponding author. Tel.: +91 484 2577404; fax: +91 484 2577595.
E-mail address: mraiyer@gmail.com (M.R. Anantharaman).

0925-8388/$ – see front matter © 2009 Elsevier B.V. All rights reserved.
doi:10.1016/j.jallcom.2009.09.077

ration of nanofillers in polymer matrix has proved to give better reinforcing properties than their ceramic counter parts [12]. In the present study, we have synthesized polycrystalline nickel ferrite nanoparticles by sol–gel method, and incorporated in natural rubber matrix. The dielectric and magnetic properties of rubber ferrite nanocomposites are studied by varying the filler concentrations in the matrix. The frequency dispersion of complex permittivity and permeability was examined using cavity perturbation technique [13]. This technique is non-destructive, simple and requires specimen of relatively small size. Maxwell-Garnett mixture equation was employed to evaluate effective permittivity and permeability of the composite sheets. Results are compared with the experimental values. Good agreement of the experimental results with Maxwell-Garnett effective medium theory can help in engineering the material constants to develop good absorber. The attenuation constant and reflection loss of the composites are determined from the measured permittivity and permeability values.

2. Materials and methods

2.1. Synthesis and characterization of natural rubber–nickel ferrite nanocomposites

Nickel ferrite particles were synthesized by using a modified sol–gel method [14]. Analytical grade $Fe(NO_3)_3{\cdot}9H_2O$ and $Ni(NO_3)_2{\cdot}6H_2O$ were taken in a 2:1 molar ratio and dissolved in a minimum amount of ethylene glycol at room temperature. The saturated solution was heated at $60 \pm 5\,^{\circ}C$ for 2 h to form a wet gel. This was further dried at $100 \pm 5\,^{\circ}C$ leading to self-ignition to produce fluffy nickel ferrite nanoparticles. They were then homogenized in a high energy ball milling unit (Fritsch Planetary Micromill 'Pulverisette 7') at 200 rpm for 10 min.

Nickel ferrite nanoparticles were incorporated in a natural rubber (grade ISNR-5, supplied by Rubber Research Institute of India, Rubber Board, Kottayam) matrix according to a specific recipe formulated by exhaustive experimental iteration. Blending was carried out in a Brabender Plasticorder (torque rheometer model PL 3S) at 70 °C with appropriate amount of nickel ferrite, zinc oxide, stearic acid, triphenyl quinone, N-cylohexyl benzthiazyl sulphenamide and sulphur along with natural rubber. Composites with different weight percentage of nickel ferrite (0–120 phr in steps of 20; phr—parts per hundred parts of rubber) were prepared. They were then homogenized in a two roll mill (15 cm × 33 cm) with a 0.8 mm nip gap as per ASTM standards [ASTM D 3182-89(2001)]. The cure time of the rubber compound was determined after aging for 24 h. The compound was moulded in an electrically heated hydraulic press having 45 cm × 45 cm platens at a pressure of 140 kg/cm^2 in a standard mould up to their respective cure time at 150 °C. The samples were labeled as *NRBlank* (Blank Natural Rubber) and *NRNFx* (*x* denotes phr of nickel ferrite incorporated in natural rubber).

Nickel ferrite as well as rubber ferrite composites were characterized using X-ray diffractometer (Rigaku Dmax-2C diffractometer with nickel filter using Cu Kα radiation of wavelength λ = 1.54 Å). Transmission electron microscopy (PHILIPS CM200 operating at 20 kV) was employed to determine the particle size of nickel ferrite filler particles. The room temperature magnetic properties of the composites were studied using a vibrating sample magnetometer (EG&G PAR 4500).

2.2. Evaluation of complex dielectric permittivity and magnetic permeability using cavity perturbation technique

Complex dielectric permittivity and magnetic permeability were determined with the help of a vector network analyzer in the S (2–4 GHz, Rohde & Schwarz-ZVB4) and X-band (8–12 GHz, Agilent-8510C) by employing the cavity perturbation technique. Rectangular cavities of dimensions 3.4 cm × 7.2 cm × 30.8 cm and 1 cm × 2.3 cm × 15.1 cm with a narrow line slot to insert the sample material into the cavity were fabricated. Calibration was performed by the method of through-open-short-match (TOSM) before carrying out the measurements. The microwave cavity was perturbed at different frequencies corresponding to different TE_{10n} modes.

The flexible nanocomposite samples prepared in the form of sheets of ~2 mm thickness were cut into thin rectangular strips of length ~4 cm. Complex dielectric permittivity ($\varepsilon' - i\varepsilon''$) and magnetic permeability ($\mu' - i\mu''$) were determined by measuring the shift in resonant frequency and the change in quality factor of a perturbed microwave cavity by inserting a sample of dimension 1 mm × 2 mm × 4 cm into the cavity at the maximum electric and magnetic field positions, respectively.

Real and imaginary part of complex dielectric permittivity for the material inserted in a rectangular cavity is given by [15–17],

$$\varepsilon' = \frac{V_c(f_c - f_s)}{2V_s f_s} + 1 \quad (1)$$

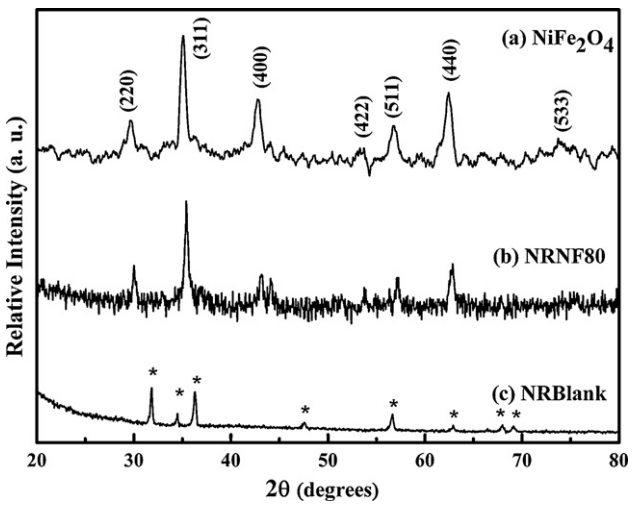

Fig. 1. X-ray diffraction pattern of (a) $NiFe_2O_4$, (b) NRNF80 and (c) NRBlank.

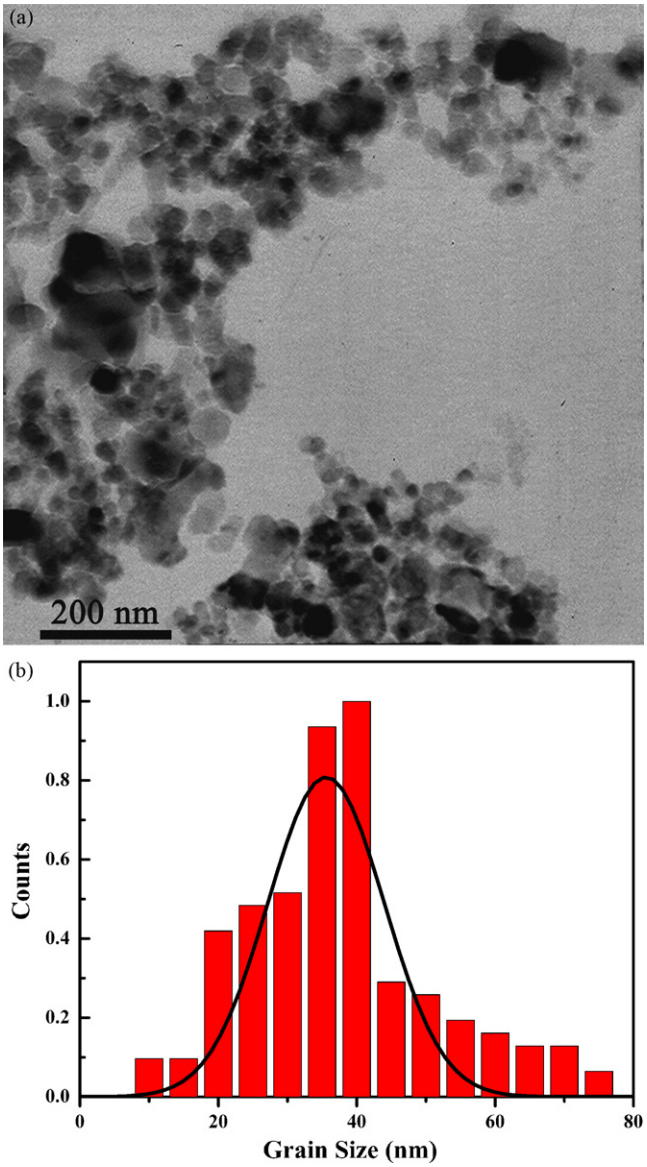

Fig. 2. (a) TEM image of $NiFe_2O_4$ and (b) normalized Gaussian fit of grain size distribution.

$$\varepsilon'' = \frac{V_c}{4V_s}\left(\frac{1}{Q_s} - \frac{1}{Q_c}\right) \quad (2)$$

where V_s and V_c are the volume of the material and cavity, respectively. f_s and f_c are the resonance frequencies with and without the material while Q_s and Q_c are the corresponding quality factors of the cavity, given by

$$Q_s = \frac{f_s}{f_c - f_s}, \qquad Q_c = \frac{f_c}{f_c - f_s} \quad (3)$$

The real and imaginary parts of the complex permeability can be obtained from the relation [17]

$$\mu' = 1 + \frac{\lambda_g^2 + 4a^2}{8a^2}\frac{f_c - f_s}{f_s}\frac{V_c}{V_s} \quad (4)$$

$$\mu'' = \frac{\lambda_g^2 + 4a^2}{16a^2}\left(\frac{1}{Q_s} - \frac{1}{Q_c}\right)\frac{V_c}{V_s} \quad (5)$$

Here a (a = 3.4 cm for S-band and a = 1 cm for X-band) is the height of the cavity and λ_g is the guided wavelength. For TE_{10n} mode, $\lambda_g = 2d/p$ where d is the length of the cavity and p = 1, 2, 3, 4, ...

3. Results and discussion

3.1. Structural and magnetic properties of composites

X-ray diffraction (XRD) pattern of $NiFe_2O_4$, NRNF80 and NRBlank are depicted in Fig. 1a–c. The characteristic diffraction peaks of $NiFe_2O_4$ (ICDD file no. 01-74-2081) observed in the nickel ferrite powder and composite confirms the formation of pure inverse spinel structure of the nickel ferrite filler material. From the XRD pattern, average particle size was evaluated using Debye Scherrer's formula [18] and is found to be 32 nm. Size of nickel ferrite particles were also determined from the transmission electron micrograph (Fig. 2a). From the normalized Gaussian fit (Fig. 2b) of size distribution, an average particle size of 35 nm was obtained. This is consistent with the particle size estimated from XRD pattern. Diffraction peaks found in NRBlank (marked as '*' in Fig. 1c) are emanating from the unreacted curatives present in the composite. These peaks disappear at higher filler concentration (Fig. 1b), since characteristic peaks of crystalline nickel ferrite becomes more prominent.

The room temperature hysteresis curve of nickel ferrite and RFCs are shown in Fig. 3a. For nickel ferrite, the hysteresis loop parameters like saturation magnetization (M_s), coercivity (H_c) and magnetic remanence (M_r) are found to be 44.1 emu/g, 111 Oe and 6.3 emu/g, respectively. A lower value of saturation magnetization of nickel ferrite when compared to the bulk (56 emu/g) [19] can be attributed to finite size effects [14] occurring at the nanoregime. The saturation magnetizations of RFCs are calculated using simple mixture equations [20] and are found to be in good agreement with the experimental values as shown in Fig. 3b. This indicates the non-interacting nature of filler with the matrix.

3.2. Complex dielectric permittivity of the composite

The variation of complex dielectric permittivity of RFCs at different frequencies in the S-band is shown in Fig. 4. The dielectric permittivity (ε') and dielectric loss (ε'') are found

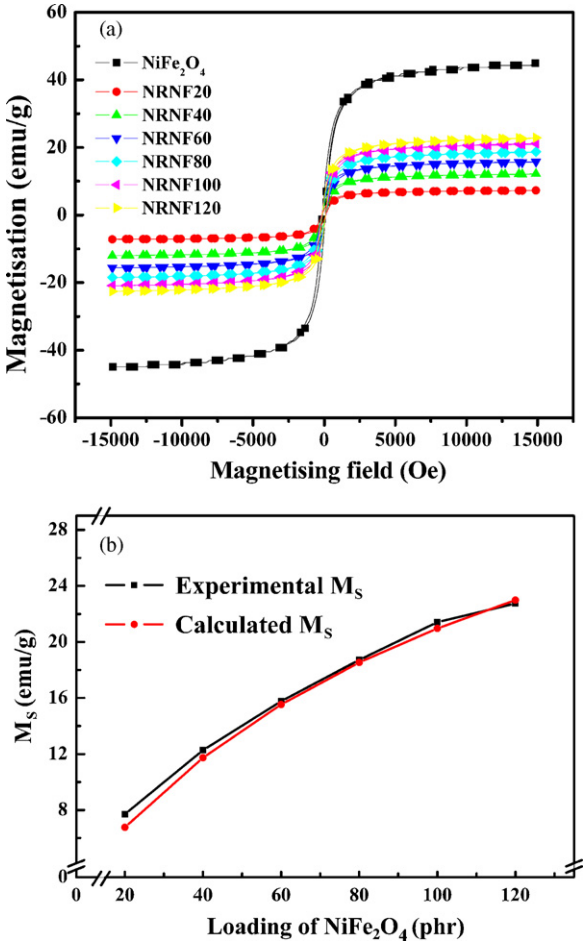

Fig. 3. Room temperature M–H curve for (a) $NiFe_2O_4$ and rubber ferrite composites with different loading of nickel ferrite; (b) variation of M_s with nickel ferrite loading in natural rubber composite.

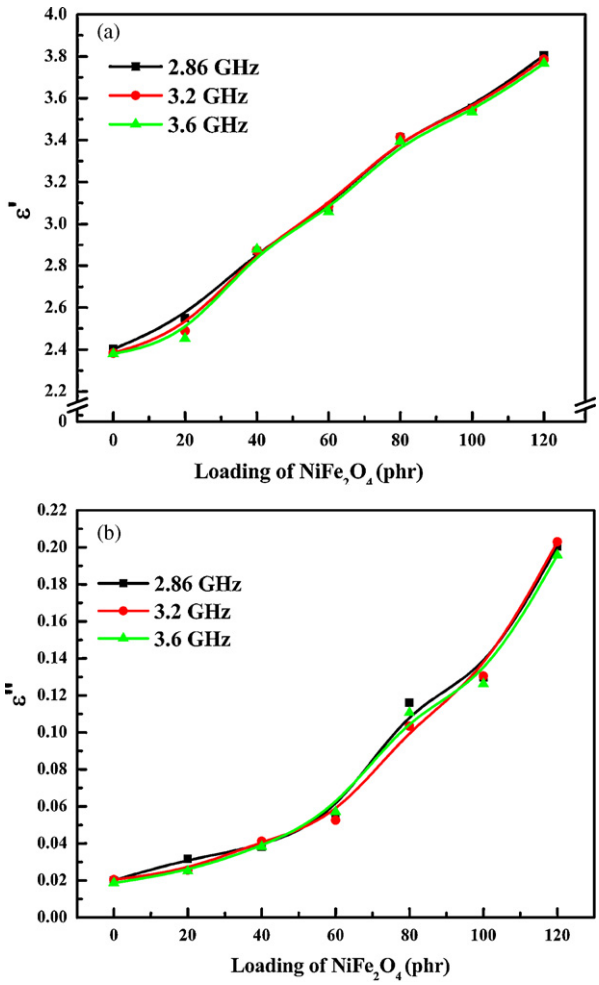

Fig. 4. Variation of (a) ε' and (b) ε'' with loading of nickel ferrite.

to increase with filler loading. Different types of polarization mechanisms (electronic/ionic/molecular/interfacial) contribute to dielectric permittivity of materials [21]. Electronic and atomic/ionic polarizations occur at optical frequencies [22] while dipolar and interfacial polarizations play a main role at lower frequencies. Since natural rubber is a non-polar material, nickel ferrite plays prominent role in deciding about the permittivity of the composites.

Iron and nickel ions in $NiFe_2O_4$ form electric dipoles with the surrounding O^{-2} and contribute to ε' through dipolar polarization. As the weight percentage of nickel ferrite in rubber matrix increases more number of dipoles become available in the composite. This enhances the dielectric permittivity of the composite with higher content of nickel ferrite. Incorporation of nickel ferrite nanoparticles (NRNF120) increased the dielectric permittivity of the elastomer from 2.38 to 3.8 (Fig. 4a). This is similar to the results reported in ferrite/EPDM rubber composite [8,23]. In addition to dipolar polarization, interfacial polarization as well as hopping of electrons within the grain and across the grain boundaries, contribute to complex dielectric permittivity [24,25].

The effective dielectric permittivity (ε_{eff}) of the composites is calculated from the two component structure dependent Maxwell-Garnett mixture equation given by [8,26],

$$\varepsilon_{eff} = \varepsilon_m \frac{2\varepsilon_m(1-v) + \varepsilon_i(1+2v)}{\varepsilon_m(2+v) + \varepsilon_i(1-v)} \quad (6)$$

Here ε_{eff} is the effective permittivity of the composite, ε_m is the permittivity of the insulating host medium (natural rubber), ε_i is the permittivity of the inclusion (nickel ferrite) and v is the volume fraction of the inclusion (nickel ferrite). When the permittivity of the inclusion is much higher than the medium, Maxwell-Garnett theory breaks for all frequencies. By factorizing ε_i and applying the condition $\varepsilon_i \gg \varepsilon_m$, we have [27]

$$\varepsilon_{eff} = \varepsilon_m \frac{1+2v}{1-v} \quad (7)$$

Fig. 5 shows the plot of measured and calculated effective permittivity at different frequencies as a function of ferrite content. There is a good agreement between the two plots. Maximum deviation of the measured permittivity from the calculated value is only 3.2%. However the dielectric permittivity is found to be a constant within the measured frequency range.

3.3. Complex magnetic permeability of the composite

When microwave propagates through a material, losses occur due to the time dependent magnetic field represented by the complex permeability. The real part of relative permeability (μ') represents the reactive portion while the imaginary part (μ'') describes the magnetic losses. Fig. 6 depicts the variation of μ' and μ'' with frequency for the composites with different ferrite concen-

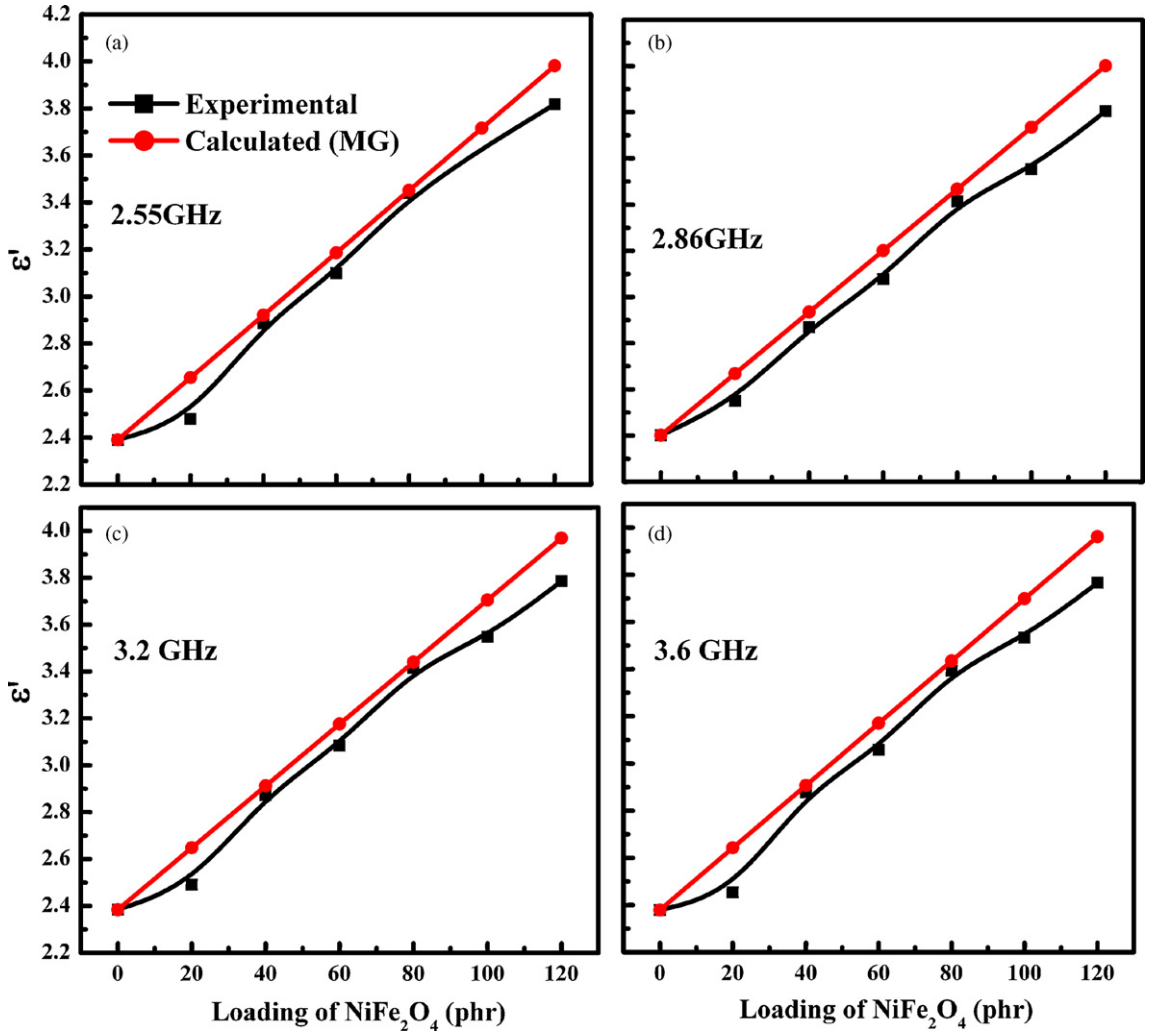

Fig. 5. Measured and calculated (Maxwell-Garnett mixture equation) effective permittivity of rubber ferrite composites at different frequencies (a) 2.55 GHz, (b) 2.86 GHz, (c) 3.2 GHz, and (d) 3.6 GHz.

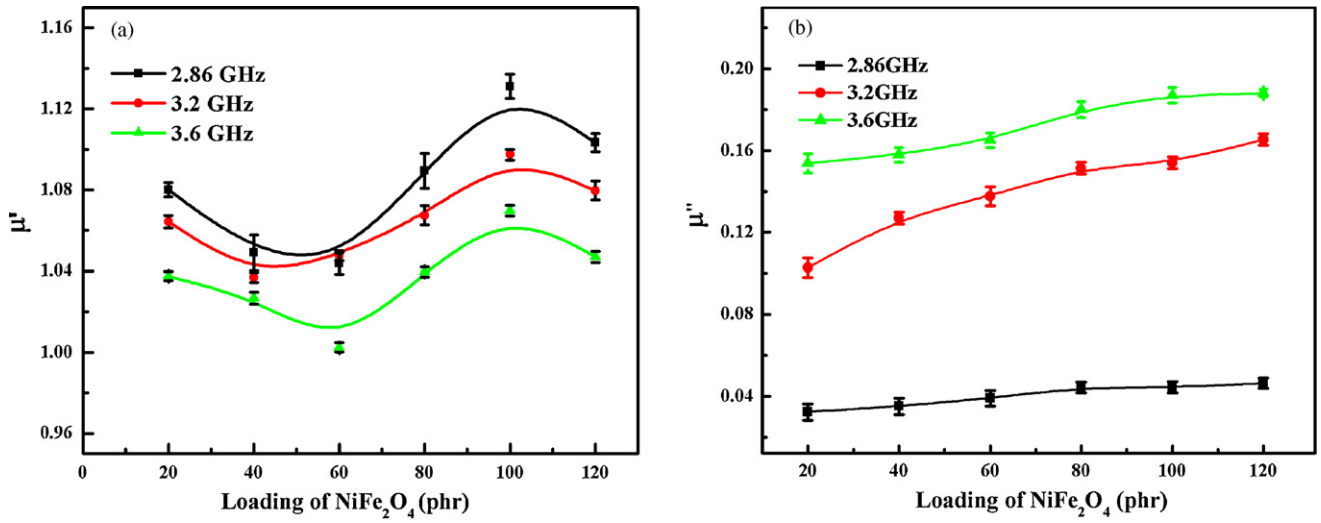

Fig. 6. (a) Real and (b) imaginary part of complex permeability of nickel ferrite rubber composite at different frequencies.

trations. The permeability is found to decrease with frequency and increase with filler loading.

Permeability dispersion observed in ferrite is due to two magnetization processes: domain wall motion and spin rotation [28]. The permeability (μ) can be expressed as $\mu' = 1 + \chi_{spin} + \chi_{domain}$. But intrinsic rotational susceptibility (χ_{spin}) and domain wall susceptibility (χ_{domain}) in turn is related to the square of saturation magnetization (M_s) [29]. Thus permeability has a direct dependence on M_s. Hence higher value of M_s is one of the reasons for improved permeability for composites with higher filler content. For single domain particles (less than their critical diameter), the main contribution for increased permeability is solely from spin rotation, while the domain wall motion can be neglected. However the composites are found to have lower permeability values when

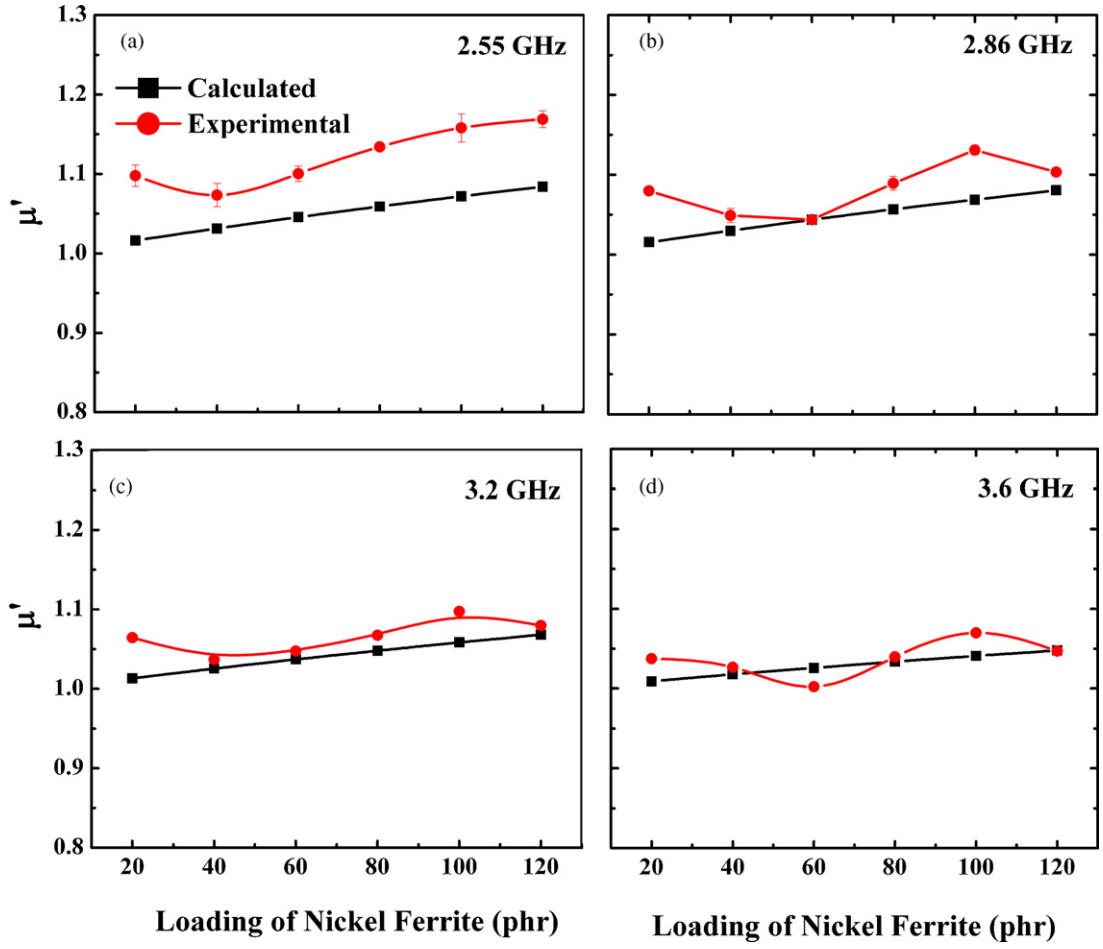

Fig. 7. Measured and calculated (Maxwell-Garnett mixture equation) effective permeability of rubber ferrite composites at different frequencies (a) 2.55 GHz, (b) 2.86 GHz, (c) 3.2 GHz, and (d) 3.6 GHz.

compared to that of pure ferrites. This is because the ferrite grains are embedded in rubber matrix. The nonmagnetic rubber matrix causes a discontinuity in the composite giving way to demagnetizing fields thus reducing the permeability [27] at low filler content.

A gradual increase in the dissipative part of permeability (μ') is observed with increase in frequency (Fig. 6b) which is pronounced in composite with higher ferrite concentration (NRNF120). This enhancement of magnetic loss with loading of nickel ferrite will improve the electromagnetic interference shielding effects.

The observed permeability of the composite is compared (Fig. 7) with the values evaluated using the Maxwell-Garnett mixture equation given by

$$\mu_{eff} = \mu_m \frac{2\mu_m(1-v)+\mu_i(1+2v)}{\mu_m(2+v)+\mu_i(1-v)} \quad (8)$$

Here μ_{eff} is the effective permeability of the composite, μ_m (=1) is the permeability of the host medium (natural rubber), μ_i is the permeability of the inclusion (nickel ferrite) and v is the volume fraction of inclusion (nickel ferrite). The discrepancy between the measured and calculated values is attributed to magnetic interactions occurring between the grains of nickel ferrite. This interaction increases with loading of filler. Also, factors like shape of inclusions, orientation and alignment of moments of inclusions and morphology of the composite affect the frequency response of permeability in a composite [30].

3.4. Evaluation of attenuation constant and reflection loss

Electromagnetic wave energy can be completely absorbed and dissipated to heat through magnetic and dielectric losses. This can be quantified by the attenuation constant and reflection loss which signifies the effectiveness of an absorber material. For a good microwave absorbing material, the electromagnetic wave entering should be attenuated completely. The attenuation constant (α), which is a measure of effectiveness of an absorber material [22], is estimated from the measured permittivity and permeability values using Eq. (9) (Fig. 8a).

$$\alpha = \frac{\sqrt{2}\pi f}{c}\sqrt{(\mu''\varepsilon'' - \mu'\varepsilon') + \sqrt{(\mu''\varepsilon'' - \mu'\varepsilon')^2 + (\varepsilon'\mu'' + \varepsilon''\mu')^2}} \quad (9)$$

α is found to increase with frequency as well as ferrite content in the composite. It is to be noted that at 2.55 GHz the attenuation constant is only 1.4 for NRNF20 whereas a maximum value of ~18 is obtained for NRNF120 at 3.6 GHz. This suggests the improvement in shielding of the RFCs at higher frequencies.

The reflection loss as a function of normalized input impedance (Z_{in}), can be expressed as

$$\text{Reflection loss (dB)} = 20\log\left|\frac{Z_{in}-1}{Z_{in}+1}\right| \quad (10)$$

Here, the input impedance (Z_{in}) is given by $Z_{in} = (\mu_r/\varepsilon_r)^{1/2}\tanh[j(2\pi fd/c)(\mu_r\varepsilon_r)^{1/2}]$, where ε_r and μ_r are the complex permittivity and permeability respectively of the composite medium. f is the frequency, d is the thickness of the absorber and c is the velocity of light in free space. To obtain low reflection, impedance matching has to be satisfied, i.e., μ'/ε' should be close to unity. But for most of the magnetic materials, μ' is less than ε' at high frequencies constraining the choice of ideal absorber material for the frequency of interest. Improving microwave permeability is difficult and hence lower values of ε'', higher values of μ'' and appropriate values of μ' and ε' are sort after to develop a good microwave absorbing material.

The measured complex permittivity and permeability values in the S-band were interpolated using computer assisted software. From this the frequency dependence of reflection loss was calculated using Eq. (10). Reflection loss minima of −5.9 dB at 3.2 GHz was obtained for 12 mm thick NRNF120 composite sheet (Fig. 8b). Moreover a shift in minimum reflection loss frequency is observed with increase in thickness. This is conclusive from the quarter wave principle [22]. When the electromagnetic wave is incident on an absorber backed by metal plate, a part of it is reflected for the air–absorber interface while some part is reflected from the absorber–metal interface. These two reflected waves are out of phase by 180° and cancel each other at the air–absorber interface when the quarter wave thickness criteria is satisfied, i.e., $t_0 = (c/4f)\left(1/\sqrt{\mu'\varepsilon'}\right)(1+(1/8)\tan^2\delta_\mu)^{-1}$ [7] where t is the absorber layer thickness, c the velocity of light, f the frequency and $\tan\delta_\mu = \mu''/\mu'$, the magnetic loss. Since $t \propto (1/f)$, above criterion is satisfied at increased sample thickness for lower frequencies.

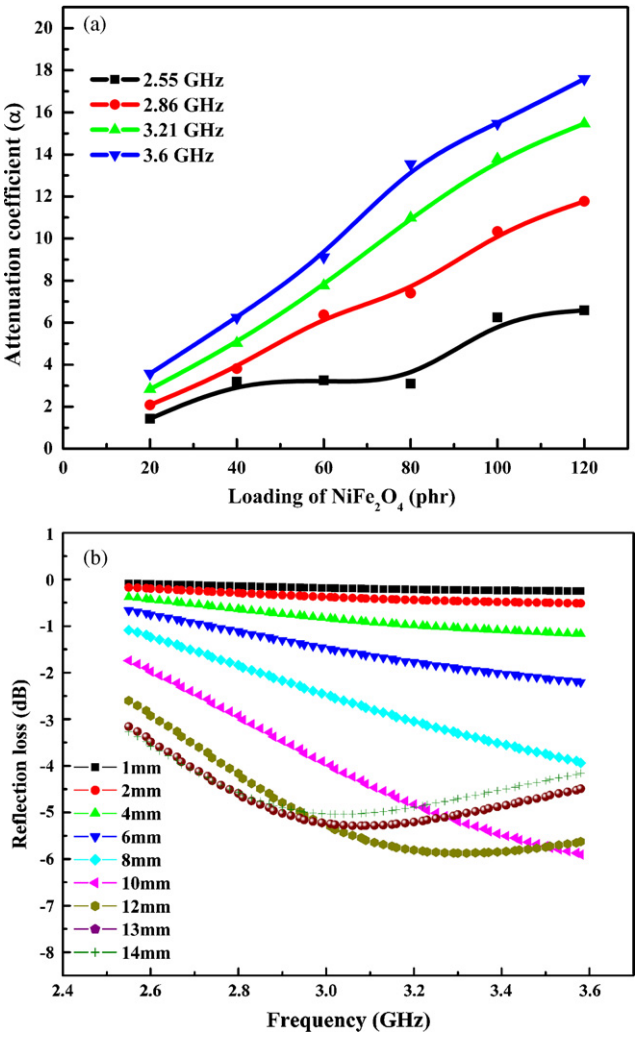

Fig. 8. (a) Variation of attenuation constant with filler concentration and (b) variation of reflection loss with thickness in the S-band.

The X-band permittivity and permeability of selected composites (NRNF20, NRNF80 and NRNF120) were measured and their corresponding reflection losses were simulated for a thickness of 12 mm. ε' is found to be 2.4, 2.9 and 3.7 while ε'' is obtained as 0.02, 0.07 and 0.22 respectively for NRNF20, NRNF80 and NRNF120 samples. The measured value of μ' is 1.02, 1.04 and 1.06 whereas μ'' is 0.04, 0.08 and 0.14 respectively for NRNF20, NRNF80 and NRNF120. The reflection loss of the composite is found to depend on the filler concentration. Simulations gave a minimum reflection loss of −16 dB at 9.5 GHz for NRNF120 with an absorber thickness of

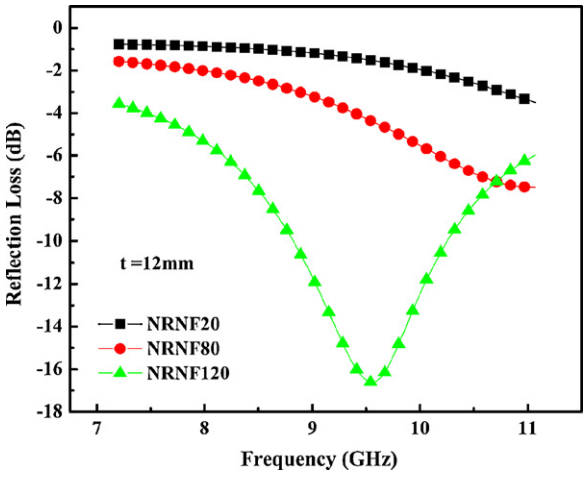

Fig. 9. Reflection loss evaluated for NRNF20, NRNF80 and NRNF120 with a sheet thickness of 12 mm in the X-band.

12 mm (Fig. 9). As reported in literature [25], the minimum reflection frequency is found to shift towards lower frequency region with the increase in filler content. Tailoring the complex dielectric permittivity and magnetic permeability of the composites will aid in obtaining improved wave absorption in the materials based on natural rubber.

Mechanical properties of the composites were determined by measuring their tensile strength (universal testing machine-Shimadzu model SPL 10 KN) and hardness (Shore A-Durometer ASTM D 2240-03). Dumbbell shaped specimens were punched out from the composite sheets using ASTM D-type and subjected to stress–strain measurements. The tensile strength declined from 22 to 12 MPa when the filler concentration was increased, but remained well within the limits of commercial elastomers. Hardness of the elastomer increased from 12 to 37 (Shore A). Good mechanical properties clubbed with microwave absorbing properties of RFCs make them useful as flexible microwave absorbing materials.

4. Conclusions

Nickel ferrite nanoparticles of average grain size ~35 nm were prepared, and incorporated in a rubber matrix to obtain rubber ferrite nanocomposites with different ferrite concentrations. Flexible, light weight composites with adequate mechanical properties could be easily moulded into desired shape. The complex permittivity and permeability of the composites were measured using cavity perturbation method. Maxwell-Garnett model is found to fit well with the experimental results of effective permittivity and permeability. The attenuation constant increased with frequency as well as filler loading suggesting better absorption at higher frequencies. This was further examined by evaluating the reflection loss for various thicknesses at different frequencies. A minimum reflection loss of −5.9 dB in the S-band is obtained for 12 mm thick 120 phr nickel ferrite loaded natural rubber composite. Extending the simulation to higher frequencies suggest a reflection loss of up to −16 dB at 9.5 GHz for 12 mm thick NRNF120 composite. These microwave characteristics integrated with superlative mechanical properties of natural rubber are desirable for using RFCs as absorbers in the high frequency regime.

Acknowledgements

This work was supported by Kerala State Council for Science, Technology and Environment (C.O. No. (T)/159/SRS/2004/CSTE dated: 25-09-2004), Kerala, India, and All India Council for Technical Education (File No. 8023/RID-73/2004-05 dated: 29-03-2005), Government of India. VS acknowledges University Grants Commission (U.O. No. Ac. C2/RFSMS/1199/07 dated 26.10.2007), for financial assistance in the form of a fellowship. Authors thank T. K. Gundu Rao, IIT Bombay, India for carrying out TEM studies.

References

[1] O.P. Gandhi, Microwave Engineering and Applications, Pergamon Press, 1989.
[2] M.R. Anantharaman, S. Sindhu, S. Jagatheesan, K.A. Malini, P. Kurian, J. Phys. D: Appl. Phys. 32 (15) (1999) 1801.
[3] S. Kolev, A. Yanev, I. Nedkov, Phys. Status Solidi C 3 (5) (2006) 1308.
[4] N.N. Al-Moayed, M.N. Afsar, U.A. Khan, S. McCooey, M. Obol, IEEE Trans. Magn. 44 (7) (2008) 1768.
[5] G. Viau, F. Fievet-Vincent, F. Fievet, P. Toneguzzo, F. Ravel, O. Acher, J. Appl. Phys. 81 (6) (1997) 2749.
[6] X. Yu, G. Lin, D. Zhang, H. He, Mater. Des. 27 (2006) 700.
[7] B. Zhang, Y. Feng, J. Xiong, Y. Yang, H. Lu, IEEE Trans. Magn. 42 (7) (2006) 1778.
[8] K.H. Prema, P. Kurian, M.R. Anantharaman, M.N. Suma, M. Joseph, J. Elastom. Plast. 40 (2008) 331.
[9] M.R. Anantharaman, K.A. Malini, S. Sindhu, E.M. Mohammed, S.K. Date, S.D. Kulkarni, P.A. Joy, P. Kurian, Bull. Mater. Sci. 24 (6) (2001) 623.
[10] C.M. Blow, C. Hepburn, Rubber Technology and Manufacture, second ed., Butterworths, London, 1982.
[11] A.J. Baden Fuller, Ferrites at Microwave Frequencies, Peter Peregrinus (Ltd.), London, 1987.
[12] C. Piña-Hernández, L. Hernández, L.M. Flores-Vélez, L.F. del Castillo, O. Domínguez, J. Mater. Eng. Perform. 16 (4) (2007) 470.
[13] B. Viswanathan, V.R.K. Murthy, Ferrite Materials Science and Technology, Springer-Verlag, London, 1990.
[14] M. George, A.M. John, S.S. Nair, P.A. Joy, M.R. Anantharaman, J. Magn. Magn. Mater. 302 (1) (2006) 190.
[15] A. Verma, D.C. Dube, IEEE Trans. Instrum. Meas. 54 (2005) 2120.
[16] T.N. Narayanan, V. Sunny, M.M. Shaijumon, P.M. Ajayan, M.R. Anantharaman, Electrochem. Solid-State Lett. 12 (4) (2009) K21.
[17] M. Lin, Y. Wnag, M.N. Afsar, Infrared and Millimeter Waves and 13th International Conference on Terahertz Electronics, Williamsburg, VA, 2005, p. 62.
[18] C. Suryanarayana, M. Grant Norton, X-ray Diffraction, Plenum Press, 1998.
[19] V. Sepelák, K. Tkáová, V.V. Boldyrev, S. Wißmann, K.D. Becker, Physica B 617 (1997) 234.
[20] E. Muhammad Abdul Jamal, P.A. Joy, P. Kurian, M.R. Anantharaman, Mater. Sci. Eng., B 156 (2009) 24.
[21] J. Xie, M. Han, L. Chen, R. Kuang, L. Deng, J. Magn. Magn. Mater. 314 (1) (2007) 37.
[22] A.N. Yusoff, M.H. Abdullah, S.H. Ahmad, S.F. Jusoh, A.A. Mansor, S.A.A. Hamid, J. Appl. Phys. 92 (2002) 876.
[23] F. Yongbao, Q. Tai, S. Chunying, L. Xiaoyun, Microwave Conference Proceedings APMC 2005. Asia-Pacific Conference Proceedings, vol. 2, 2005, p. 4.
[24] Z. Haijun, L. Zhichao, Y. Xi, Z. Liangying, W. Mingzhong, Mater. Sci. Eng., B 97 (2003) 160.
[25] H. Zhao, X. Sun, C. Mao, J. Du, Physica B 404 (2009) 69.
[26] M. Wu, H. Zhang, X. Yao, L. Zhang, J. Phys. D: Appl. Phys. 34 (2001) 889.
[27] K. Bober, R.H. Giles, J. Waldman, Int. J. Infrared Millimeter Waves 18 (L) (1997) 101.
[28] J.P. Bouchaud, P.G. Zerah, J. Appl. Phys. 67 (1989) 5512.
[29] T. Nakamura, J. Magn. Magn. Mater. 168 (3) (1996) 285.
[30] M.Y. Koledintseva, P.C. Ravva, R.E. DuBrofff, J.L. Drewniak, K.N. Rozanov, B. Archambeault, Proc. IEEE Int. Symp. Electromag. Compat., vol. 1, 2005, p. 169.